

PACS numbers: 52.57.–z; 52.38.Mf
DOI: 10.1070/QE2007v037n10ABEH013615

Laser acceleration of thin foils

V.I. Vovchenko, I.K. Krasyuk, P.P. Pashinin, A.Yu. Semenov

***Abstract*. A method for studying the characteristics of laser-induced ablative acceleration of thin foils is described. The method is based on the electrocontact measurement of the time of foil flight through base distances in the air atmosphere. Results of experiments on the laser acceleration of foils in cylindrical and conical channels for laser radiation intensities up to 2×10^{11} W cm^{-2} are presented. The results obtained were used in experiments to determine the split-off strength of aluminium targets at high strain rates, the accelerated aluminium foils being used as strikers.**

Keywords: *laser radiation, ablative pressure, foil acceleration, cylindrical and conical targets, strain rate, split-off strength.*

1. Introduction

The laser-induced acceleration of foils is a part of experiments for the production of dense high-temperature plasmas in shell conical targets. Theoretical investigations carried out earlier suggest that the crucial role in the production of high-temperature plasma in this case is played by cumulative effects inside the conical target, which take place upon interaction of the moving foil with the wall of the conical cavity [1]. The foils accelerated by laser radiation may also be used as strikers in experiments on the study of thermal and mechanical properties of a material under extreme conditions. In this case, the interaction between the striker and the target under study can produce higher pressures and strain rates than upon the direct target exposure to the laser radiation itself.

The aim of the present work was to study experimentally the characteristics of laser-induced foil acceleration in cylindrical and conical channels and to apply the accelerated foils in experiments on the initiation of splitting-off at high strain rates.

A laser pulse incident on a foil produces ablation of a part of the foil material accompanied by the formation of a plasma stream moving in the opposite direction to the laser beam. This gives rise to the reactive recoil momentum (ablative pressure) acting on the unevaporated part of the foils. In the present work, the foil mass and velocity after laser ablation and acceleration were determined by the method of their deceleration in a gas atmosphere [2]. This method is based on the electrocontact measurement of the time of foil flight through base distances. Below, we give a complete description of the deceleration method for measuring the velocity and unevaporated mass of the foils accelerated by ablative laser pressure, describe experiments on foil acceleration, and present the data obtained. We also report the results of experiments employing accelerated aluminium foils as strikers for studying the split-off strength of aluminium.

V.I. Vovchenko, I.K. Krasyuk, P.P. Pashinin, A.Yu. Semenov
A.M. Prokhorov General Physics Institute, Russian Academy of Sciences, ul. Vavilova 38, 119991 Moscow, Russia;
e-mail: krasyuk@kapella.gpi.ru

Received 2 May 2007; revision received 28 June 2007
Kvantovaya Elektronika **37** (10) 897–902 (2007)
Translated by E.N. Ragozin

2. Determination of characteristics of laser-induced acceleration of foils by the method of their deceleration in the air atmosphere

In a simplified one-dimensional formulation, the problem of striker deceleration in a gas may be formulated as follows: a striker of thickness h with a density ρ_m and a velocity u_0 collides with a semi-infinite stationary gas layer with an initial density ρ_0 at a pressure p_0. The subsequent collision produces shock waves in the striker and the gas. The shock wave in the striker is reflected from its free boundary in the form of a rarefaction wave, which arrives at the interface with the gas and causes the striker deceleration. A complex wave picture of the gas flow appears, and the striker deceleration is determined both by the gas hydrodynamics and the wave motion of the striker material.

For a rigid striker, when the shock wave is 'weak' (remaining 'strong' for the gas), the perturbations introduced by collisions with the gas may be assumed acoustic. In this case, the exact solution may be obtained from acoustic equations

$$u_t + \frac{p_x}{\rho_m} = 0, \quad p_t + \rho_m c_m^2 u_x = 0.$$

Here, u is the velocity of the medium (the striker) through which the 'weak' shock wave propagates; p is the pressure in this medium (more precisely, u and p are the small perturbations of the velocity and pressure from their values in the unperturbed medium caused by the propagation of shock waves); t is the time; x is the spatial coordinate; the quantities with the subscripts t and x are the partial derivatives with respect to the variables t and x; and c_m is the sound speed in the striker. The solution of the

formulated problem may be found with the help of Riemann invariants [3].

Let us assume that at the instant of time t the right Riemann invariant $J_+(t) = u(t) + p(t)/(\rho_m c_m)$ arrives at the striker – gas interface. If the pressure at the contact surface is $p(t)$ and the interface velocity is $u(t)$, we have

$$[J_+(t) + J_-(t)]/2 = u(t), \quad \rho_m c_m [J_+(t) - J_-(t)]/2 = p(t),$$

Where $J_-(t) = u(t) - p(t)/(\rho_m c_m)$ is the left Riemann invariant. The characteristic of this invariant after reflection from the free surface of the striker, returns to the contact surface at the instant $t + 2h/c_m$:

$$\frac{1}{2}\rho_m c_m \left[J_+\left(t + \frac{2h}{c_m}\right) - J_-\left(t - \frac{2h}{c_m}\right)\right] = p\left(t + \frac{2h}{c_m}\right).$$

From the condition $p = 0$ at the free surface it follows that

$$J_+\left(t + \frac{2h}{c_m}\right) = J_-(t).$$

The above relations give the expressions

$$-\frac{1}{2}\left[J_+(t) - J_-\left(t + \frac{2h}{c_m}\right)\right] = u\left(t + \frac{2h}{c_m}\right) - u(t),$$

or

$$-\rho_m c_m \left[u\left(t + \frac{2h}{c_m}\right) - u(t)\right] = p\left(t + \frac{2h}{c_m}\right) + p(t).$$

By expanding the latter relation into a Taylor series in powers of h/c_m (as will be evident from the subsequent discussion, this quantity, which is equal to half the total time of acoustic wave transit through the striker, is short compared to the characteristic times of gas flow) and neglecting the terms of the higher order of smallness, we obtain the relation between a change in the interface velocity and pressure on it:

$$2\rho_m h \frac{du}{dt} = -2p, \quad \text{or} \quad m\frac{du}{dt} = -p, \tag{1}$$

where m is the mass of the piston (striker) per unit area.

Therefore, in the approximation accepted for determining the velocity of the striker, there is no need to know its hydrodynamics. The established relation is the boundary condition for the integration of the equations of gas motion and expresses in fact the second Newton law for the striker as a whole. The law of striker deceleration is determined by integrating simultaneously the equation of motion of the shock-compressed gas and Eqn (1) taken as the boundary condition.

By assuming that the layer of the shock-compressed gas contained between the shock wave front and the piston surface is short, i.e. assuming that the pressure profile is rectangular, we arrive at the stationary approximation. In this case, the piston velocity u and the pressure p at the piston are related by the expression:

$$p - p_0 = \rho_0 D u \tag{2}$$

at the front of a plane stationary shock wave, where D is the velocity of the shock-wave front and p_0 is the unperturbed gas pressure. For a 'strong' shock wave ($p \gg p_0$) in a gas with the effective ratio of specific heat γ, the relation [3]

$$D = \frac{(\gamma + 1)u}{2} \tag{3}$$

is fulfilled and the shock adiabat equation determining the pressure at the piston has the form

$$p(u) = \frac{(\gamma + 1)\rho_0 u^2}{2} = au^2, \tag{4}$$

where we introduced the notation

$$a = \frac{(\gamma + 1)\rho_0}{2}. \tag{5}$$

In view of Eqn (4), Eqn (1) may be written in the form

$$m\frac{du}{dt} = -au^2. \tag{6}$$

The limits of validity of the above approximations were considered in [2].

Taking into account the ablative pressure $p_a(t)$ acting on the front side of the target, which is caused by the laser pulse, Eqn (6) should be written in the form

$$m(t)\frac{du}{dt} = p_a(t) - au^2. \tag{7}$$

By replacing the real laser pulse with a rectangular laser pulse of the effective duration τ, we assume that

$$p_a = \dot{m}w = \text{const}. \tag{8}$$

Here, w is the velocity of vapour motion relative to the unevaporated part of the piston shell during ablation;

$$\dot{m} = \frac{m_0 - m_\tau}{\tau} = \frac{m_0}{T} \tag{9}$$

is the shell vaporisation rate; m_0 is the initial shell mass; m_τ is the shell mass at the instant of time $t = \tau$; and $T = \tau m_0/(m_0 - m_\tau)$ is the time of complete shell vaporisation.

Under the assumptions made above, Eqn (7) for $t \leqslant \tau$ (the active region) has the solution

$$u(t) = \left(\frac{\dot{m}w}{a}\right)^{1/2} \frac{1 - B}{1 + B}, \; B = \left(1 - \frac{t}{T}\right)^{\beta}, \; \beta = 2\left(\frac{aw}{\dot{m}}\right)^{1/2}. \tag{10}$$

For $a \to 0$, expression (10) passes to the expression for the velocity of motion of a body of variable mass in vacuum

$$u(t) = -w \ln\left(1 - \frac{t}{T}\right).$$

For times $t \geqslant \tau$ (the passive region), we have

$$u(t) = u_\tau \left[1 + \frac{au_\tau}{m_\tau}(1 - \tau)\right]^{-1}, \tag{11}$$

where u_τ is the shell velocity at the instant $t = \tau$. Here, we assume that $\tau < T$. If $\tau > T$, i.e. the shell is completely vaporised prior to the completion of the laser pulse, the shell velocity asymptotically reaches its maximum $u_{\max} = (w\dot{m}/a)^{1/2} = (p/a)^{1/2}$. In this case, the shell mass tends to zero.

Accordingly, the path propagated by the foil during the time $t - \tau$ is determined by the expression

$$l(t) = l_\tau + \frac{m_\tau}{a} \ln\left[1 + \frac{au_\tau}{m_\tau}(t - \tau)\right], \tag{12}$$

where $l_\tau = \int_0^\tau u(t)\mathrm{d}t$ is the path propagated by the foil during the laser pulse action, and $u(t)$ is specified by expression (10).

As an example we show in Fig. 1 the time dependences of the velocity $u(t)$ of motion of the 8-μm thick aluminium foil and the path $l(t)$ propagated by this foil for $u_\tau = 11$ km s^{-1} and $a = 0.014$ g cm^{-3}.

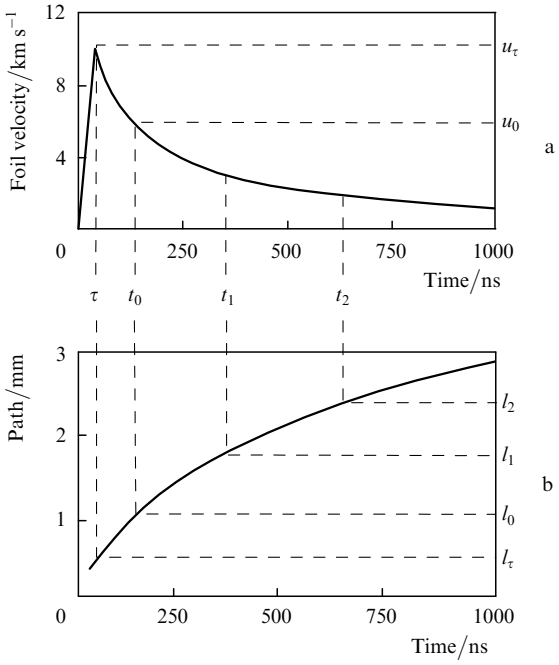

Figure 1. Time dependences of the velocity u (a) of motion of 8-μm thick aluminium foil and the path l (b) propagated by the foil for $u_\tau = 11$ km s^{-1} and $a = 0.014$ g cm^{-3} calculated from (10), (11), and (12).

Let us assume that the first contact of a sensor is located at a distance of l_0 from the initial foil position, the second one at a distance of l_1 from the first contact, and the third at a distance of l_2 from the second one. In this case, t_0, t_1, and t_2 are the instants of time at which the foil passes through the corresponding distances l_0, l_1, and l_2. Let us denote the foil velocity at the instant t_0 as u_0. Then, the foil motion in the interval between l_0 and l_2 will be described by the expressions

$$u(t) = u_0\left[1 + \frac{au_0}{m_\tau}(t - t_0)\right]^{-1}, \tag{13}$$

$$l(t) = l_0 + \frac{m_\tau}{a} \ln\left[1 + \frac{au_0}{m_\tau}(t - t_0)\right]. \tag{14}$$

Expression (14) contains two unknown quantities m_τ and u_0. To determine them, Eqn (14) can be represented in the form of a system of two equations with two unknown quantities u_0 and m_τ:

$$l_q - l_0 = \frac{m_\tau}{a} \ln\left[1 + \frac{au_0}{m_\tau}(t_q - t_0)\right], \quad q = 1, 2. \tag{15}$$

The quantities l_0, l_q, and t_0, t_q entering these equations, can be measured experimentally.

By eliminating from (15) one of the unknown quantities, for instance u_0, we arrive at a transcendental equation for the new dimensionless variable $\tilde{x} = a(l_1 - l_0)/m_\tau$:

$$f(x) = 1 + \frac{t_2 - t_0}{t_1 - t_0}\left(\mathrm{e}^{\tilde{x}} - 1\right) - \mathrm{e}^{\alpha\tilde{x}} = 0, \tag{16}$$

where we introduced the notation $\alpha = (l_2 - l_1)/(l_1 - l_0)$. The quantities u_0 and m_τ are expressed in terms of the variable $\tilde{x}$ as:

$$u_0 = \frac{l_1 - l_0}{t_1 - t_0} \frac{\mathrm{e}^{\tilde{x}} - 1}{\tilde{x}}, \tag{17}$$

$$m_\tau = q(l_1 - l_0)\tilde{x}. \tag{18}$$

Note that the quantity a in the explicit form enters only expression (18) for the calculation of m_τ. This means that to determine the velocity u_0, it is sufficient to measure only t_q and l_q ($q = 1, 2$), and to determine the mass m_τ it is also necessary to know the quantity a.

Having determined u_0 and m_τ, we can find the velocity u_τ from expression (11):

$$u_\tau = u_0\left[1 - \frac{au_0}{m_\tau}(t_0 - \tau)\right]^{-1}. \tag{19}$$

Knowing u_τ and m_τ, we can find now from (8) and (9) the rate of foil mass variation and the pressure acting on the foil during the laser-induced ablative acceleration of thin foils. In this case, the rate w of foil material vaporisation is determined from transcendental equation (10) by substituting $u(t = \tau) = u_\tau$ in it.

In experiments, the target was filled with air at an initial pressure of 1 atm ($\rho_0 = 1.2 \times 10^{-3}$ g cm^{-3}). For the piston moving with a characteristic velocity exceeding several kilometres per second, the shock wave produced in the gas is capable of ionising the shock-compressed medium [4]. The plasma produced in this case is nonideal, and therefore it is necessary to know the thermal and gas-dynamic properties of gas, which are well known for air. Figure 2 shows the pressure and temperature behind the shock-wave front and the shock-wave front velocity as functions of the velocity u, which were calculated from the data [5] for the air with an initial pressure $p_0 = 1$ atm and $T_0 = 18\,^\circ$C.

The analytic expression for the shock adiabat in the velocity range up to 25.7 km s^{-1} obtained on the basis of these data may be written in the form

$$p = \rho_0(1.13u + 0.33)u \approx 1.13\rho_0 u^2. \tag{20}$$

By comparing expressions (17) and (4), we obtain the effective ratio of specific heat for the air equal to $\gamma = 1.26$. In this case, according to (5), $a = 1.37 \times 10^{-3}$ g cm^{-3}.

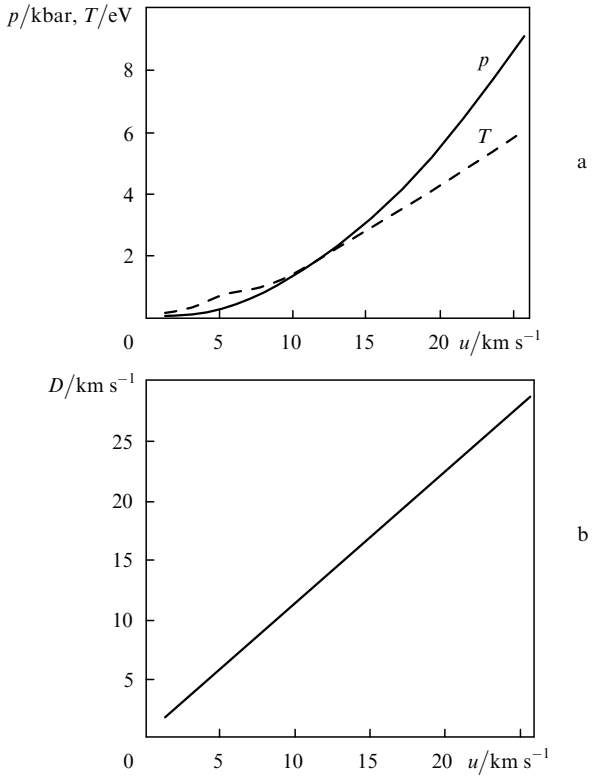

Figure 2. Pressure p and temperature T behind the shock-wave front (a) and velocity D of the shock-wave front (b) as functions of velocity u for the air for a pressure $p_0 = 1$ atm and $T_0 = 18\,^{\circ}\mathrm{C}$.

3. Experimental conditions

Experiments were performed by using a Sirius neodymium-glass laser emitting 1.06-μm, 37-ns pulses and providing an energy up to 30 J incident on the target. The laser-beam diameter was equal to 5 cm at the focusing lens, and the focal length of the lens was 40 cm. The diameter of the laser spot on the target was 1 mm; in this case, the laser radiation intensity at the target amounted to 2×10^{11} W cm^{-2}.

We studied the laser-induced acceleration of foils of aluminium (thicknesses 8 and 15 μm, density 2.7 g cm^{-3}), polyethylene terephthalate [PET, $(C_{10}O_4H_8)_n$, 14 μm, 1.38 g cm^{-3}], and a compound foil of PET (thickness 5 μm) and aluminium (thickness 8 μm). The PET foils were coated with a 0.06-μm-thick aluminium layer on the side facing the laser beam. The experiments were performed in the passive part of foil motion, i.e. following the completion of the laser pulse.

Figure 3 shows the scheme of the experimental assembly consisting of an accelerated foil, a cylindrical (shown by dashed lines) or conical channel, and an electrocontact sensor. The cylindrical channel of length l_0 in brass, in which the laser-induced acceleration of foils was performed, measured 1 mm in diameter. Experiments were performed for $l_0 = 1$, 2, 3, and 4 mm. The conical cavity in lead with a fixed length of 2 mm had an inlet diameter of 1.7 mm and an outlet diameter of 0.5 mm.

Inside the cylindrical cavity of the electrocontact sensor 1 mm in diameter there were three annular contacts; they served to record the moments of time at which the foil propagated over fixed distances l_0, $l_1 = l_0 + l_s$ и $l_2 = l_1 + l_s$, where $l_s = 1.35$ mm is the thickness of the sensor electrodes plus their separation.

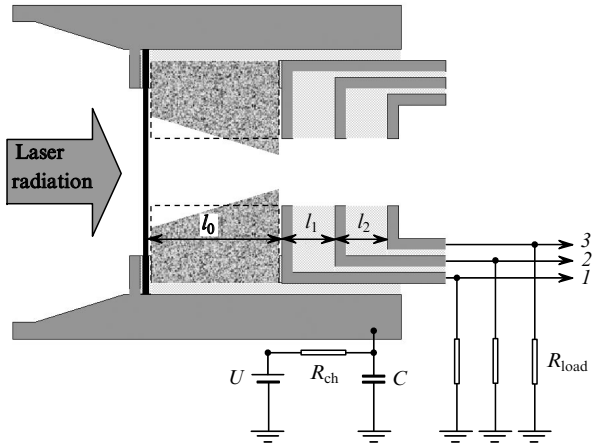

Figure 3. Scheme of the experimental assembly: (*1–3*) – oscilloscope inputs; $U = 4.5$ V; $C = 0.02$ μF; $R_{ch} = 100$ kΩ; $R_{load} = 50$ Ω; the dashed lines show the cylindrical channel accommodated in place of the conical channel.

Contacts (*1–3*) were arranged in the passive part of the foil path, i.e. where the ablation was virtually complete. The intensity of laser irradiation in our experiments was varied in the $(0.35 - 0.8) \times 10^{10}$ W cm^{-2} range. Recording was performed with digital storage 500-MHz Tektronix TDS 744A and 350-MHz LeCroy WS 432 oscilloscopes.

Figure 4 shows typical oscillograms of the signals from the electrocontact sensor, which appeared upon shorting contacts (*1–3*) to the common body of the assembly via the electric current-conducting plasma corona produced at the foil surface facing the laser beam.

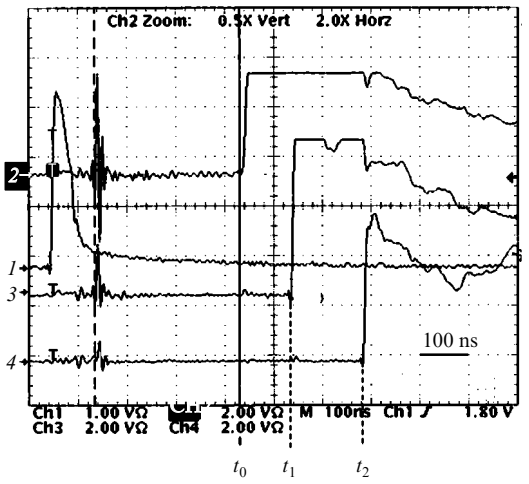

Figure 4. Typical oscillograms of the laser pulse (*1*) and the signals from the electrocontact sensor (*2–4*) in the experiments in foil deceleration in a cylindrical or conical channel.

4. Experimental results

Experimental data are collected in Table 1. The values of unevaporated foil masses and their velocities were obtained by averaging over several measurements under similar experimental conditions.

One can see from Table 1 that the foil velocities at the outlet of the conical channel are much higher than at the

Table 1. Experimental data on laser-induced foil acceleration in cylindrical and conical channels in the air atmosphere.

Accelerated foil		Channel			Foil thickness upon pulsed laser irradiation/μm	Velocity at the channel outlet/km s^{-1}
Material	Initial thickness/μm	Shape	Material	Diameter d/mm		
Al	8	Cylindrical	Cu	1	6.8	11
Al	15	Cylindrical	Cu	1	13.8	5.8
PET	14	Cylindrical	Cu	1	10.5	12.3
PET + Al	5 + 8	Cylindrical	Cu	1	1.5 + 8	8.5
Al	8	Conical	Pb	$d_{in} = 1.7$ mm, $d_{out} = 0.5$ mm	1.3	17
PET	14	Conical	Pb	$d_{in} = 1.7$ mm, $d_{out} = 0.5$ mm	1.8	28.5

outlet of the cylindrical one. In this case, the mass of the unevaporated part of the foil in the case of the conical channel is much smaller, which has so far defied explanation. The reason may supposedly lie with the manifestation of cumulative effects occurring in the interaction between the moving foil and the walls of the conical cavity.

The errors of measurement of the vaporised foil mass and its velocity were estimated from Eqn (15), into which the quantities t_q, l_q, and a were substituted taking into account the possible experimental errors. As a result, we found that the errors of measurement of the foil velocity and vaporised mass velocity were within 5 % and 30 %, respectively.

The expansion velocity w of the material vaporised during ablation, the foil vaporisation rate $\dot{m}$, and the ablative pressure p_a can be determined from expressions (8), (9), and (16) on the basis of experimental data. The following parameters were obtained for aluminium foil: $w = 70$ km s^{-1}, $\dot{m} = 7 \times 10^4$ g cm^{-2} s^{-1}, and $p_a = 50$ kbar. These values are in satisfactory agreement with the corresponding data obtained in [6] ($w = 50$ km s^{-1}, $\dot{m} = 4.7 \times 10^4$ g cm^{-2} s^{-1}, and $p_a = 36$ kbar).

5. Application of the obtained results to the study of split-off effects at high strain rates

The foils accelerated by laser pulses may be employed as strikers for the experimental determination of split-off strength of materials for strain rates which, as shown by estimates, may be much higher than for direct target exposure to the same laser radiation. In particular, when a 15-μm thick laser-accelerated foil is employed as the striker, the pulse duration at the target face does not exceed 4 ns, which is almost 10 times shorter than the duration of the laser pulse itself as well as the duration of the action of its related ablative pressure. In this case, the pressure amplitude in the striker–target collision increases by a factor of several tens compared to the amplitude of laser ablative pressure.

For a target we employed a 210-μm thick aluminium foil, which was impacted by the striker foil of thickness 8 or 15 μm. The target was placed behind the outlet of the electrocontact sensor. This enabled us to record the striker foil velocity at which there occurred splitting-off at the rear side of the target.

The measurements were made in two ways. In one of them, we recorded the threshold striker velocity at which a splitting-off at the rear side of the target occurred. In this case, the splitting-off took place at the target section where the negative pressure (tensile stress) was maximal. The amplitude of negative pressure depends on the striker velocity and thickness as well as on the target thickness. Figure 5 shows the calculated dependences of the maximum negative-pressure amplitude p in a 210-μm thick target on the striker foil velocity u for two foil thicknesses h. Also shown in Fig. 5 are the dependences of the material strain rate $\dot{V}/V_0$ on u (where $\dot{V}$ and V_0 are the specific and initial specific volumes of the target) in the plane where the maximum tensile stress $\sigma^* = -p$ is reached.

We performed numerical simulations of the shock-wave striker–target interaction with the help of a code elaborated on the basis of hydrodynamic equations in Lagrangian variables, which were supplemented with a wide-range semiempirical equation of state of aluminium [7].

As a result of a series of experiments, we found that the threshold velocity of a 15-μm-thick striker at which a splitting-off occurred a was equal to 3.6 km s^{-1}, and for an 8-μm-thick striker it was equal to 5.8 km s^{-1}. According to the dependences plotted in Fig. 5, the results were similar in both cases (dashed lines): for a strain rate $\dot{V}/V_0 = 3.6 \times 10^7$ s^{-1}, the split-off strength σ^* of aluminium was 90.4 kbar.

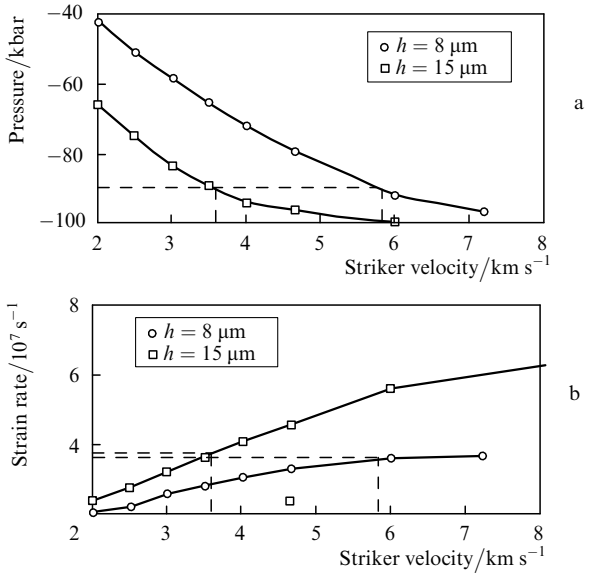

Figure 5. Maximum amplitudes of negative pressure p (a) and strain rate $\dot{V}/V_0$ (b) in a 210-μm thick aluminium target as functions of velocity u of an aluminium striker of thickness 8 and 15 μm. The dashed lines indicate the threshold striker velocities of 3.6 and 5.8 km s^{-1}, at which a splitting-off occurred.

When the foil velocity exceeded the threshold value, on the basis of experimental data we recorded the position of the splitting-off plane and the moment at which the split-off layer arrived at an additional electrocontact sensor located at a distance of 0.65 mm from the rear side of the target. Then, the values of split-off strength and strain rate were determined by the method described in [7, 8]. In these experiments, the pressure amplitude at the target face in foil – target collisions amounted to 1.4 Mbar, which is nearly 30 times higher than the ablative pressure produced by direct exposure of the target to the pulse of laser radiation.

It was eventually established that the split-off strength σ^* virtually did not change when the rate of straining $\dot{V}/V_0$ was varied from 3.6×10^7 to 8×10^7 s^{-1}, and was equal to $\sim$90 kbar. This suggests that the limiting strength of the material under investigation was reached in our experiments. The obtained value is close to the theoretical limiting strength of aluminium estimated from the minimum of the corresponding three-dimensional compression curve ($\sigma^*_{\text{theor}} = 100$ kbar) [9]. A similar result was earlier obtained in the study of the split-off strength of the AMg6M aluminium alloy by the method of direct laser irradiation of the target [7, 8].

6. Conclusions

We have developed a method for the experimental determination of the mass and velocity of thin foils accelerated under pulsed laser irradiation. The advantage of this method is that the sensor made on its basis enables monitoring kinematic foil parameters in every experiment conducted with the use of laser-accelerated foils.

We have found that the velocity of foils achieved upon their acceleration in the conical channel was higher than in the case of the cylindrical channel. The reason supposedly lies with the manifestation of cumulative effects related to the interaction of the moving foil with the walls of the conical channel. Investigations in this direction will be continued involving both experimental methods and numerical simulations.

As an application of the results obtained, we performed measurements of the split-off strength of an aluminium target at high strain rates. It has been established that the employment of foils as strikers is an efficient method for investigating the splitting-off for the limiting dynamic material strength, close to its theoretical limit.

Acknowledgements. This work was supported by the Russian Foundation for Basic Research (Grant No. 06-02-16573).

References

1. Krasyuk I.K., Semenov A.Yu., Charakhch'yan A.A. *Kvantovaya Elektron.*, **35** (9), 769 (2005) [*Quantum Electron.*, **35** (9), 769 (2005)].
2. Ageev V.G., Vovchenko V.I., Krasyuk I.K., Ni A.L., Pashinin P.P., Prokhorov A.M., Semenov A.Yu., Fortov V.E., et al. *Pis'ma Zh. Tekh. Fiz.*, **13** (1), 3 (1987).
3. Zel'dovich Ya.B., Raizer Yu.P. *Physics of Shock Waves and High-Temperature Hydrodynamic Phenomena* (New York: Academic Press, 1966, 1967; Moscow: Nauka, 1986).
4. Fortov V.E., Yakubov I.T. *Neideal'naya plazma* (Nonideal Plasma) (Moscow: Energoatomizdat, 1984) p. 102.
5. Kuznetsov N.M. *Termodinamicheskie funktsii i udarnye adiabaty vozdukha pri vysokikh temperaturakh* (Thermodynamic Functions and Shock Adiabats of the Air at High Temperatures) (Moscow: Mashinostroenie, 1965).
6. Dahmani F., Kerdia T. *Laser Part. Beam.*, **9** (3), 769 (1991).
7. Krasyuk I.K., Pashinin P.P., Semenov A.Yu., Fortov V.E. *Kvantovaya Elektron.*, **33** (7), 593 (2003) [*Quantum Electron.*, **33** (7), 593 (2003)].
8. Batani D., Vovchenko V.I., Kanel' G.I., Kil'pio A.V., Krasyuk I.K., Lomonosov I.V., Pashinin P.P., Semenov A.Yu., Fortov V.E., Shashkov E.V. *Dokl. Ross. Akad. Nauk*, **389** (3), 328 (2003).
9. Kanel' G.I., Razorenov S.V., Utkin A.V., Fortov V.E. *Udarno-volnovye yavleniya v kondensirovannykh sredakh* (Shock-Wave Phenomena in Condensed Media) (Moscow: Yanus-K, 1996) p. 201.